



Cyclic Behavior of Various Drilled Flange Beam Connected to Box Column

M. Vajdian¹, S. M. Zahrai^{2,*}, S. M. Mirhosseini¹, E. Zeighami¹

¹Department of Civil Engineering, Arak Branch, Islamic Azad University, Arak, Iran

²School of Civil Engineering, College of Engineering, University of Tehran, Tehran, Iran, also Adjunct Professor, University of Ottawa, Canada

ABSTRACT: The moment frame system is used as a lateral load resisting system against seismic loads. So far, a large body of research has been conducted on steel connections and various types of connections including Reduced Beam Section (RBS) and Drilled Flange Connection (DFC). Using RBS results in the formation of inelastic deformation in a part of the beam far from the column flange. They have studied the seismic performance of the recently developed DFC as a simple and efficient alternative to mostly used conventional RBS. In this research, the beam flange is drilled in different patterns in terms of the hole diameter. After simulating the models in Abaqus, the moment-rotation curves are extracted and analyzed numerically. Having obtained the results of the current research regarding the moment connection where beam flanges are drilled, it is evident that drilling holes in the beam flange with a clock pattern can better satisfy the flexibility expectations. Moreover, this pattern has the higher capability for plastic hinge transfer from the column face compared to the direct pattern. Additionally, this pattern can reduce the bending stress in the penetration weld of the direct beam to column connection. Thus, the clock pattern of beam flange holes performs better than the straight one.

Review History:

Received: Nov. 29, 2019

Revised: Aug. 07, 2020

Accepted: Aug. 19, 2020

Available Online: Sep. 09, 2020

Keywords:

Steel Moment Frame

Box Sections

Shear Capacity

Clock Pattern

Drilled Flange

1- Introduction

In many connections used in conventional steel structures, there is a doubt about the meeting of the above requirements for the correct beam-to-column load transfer because of inadequate elements of the connection, the inadequate resisting capacity of the connection elements, lack of continuity plates within the column section, lack of a specific panel zone for the beam-to-column moment transfer as well as basic weaknesses of the welds [1]. Since the 1960s, the steel moment frame was introduced as an appropriate structural system. Due to the open and unobstructed space between the columns, the moment frame is used in major parts of the steel structural systems as well as the design of the buildings. Unfortunately, in the early years, there was a misconception that the steel moment frame with any design, only due to its inherent features, would be able to resist the forces caused by the earthquake without any failure through yielding of its members and connections. Based on this misunderstanding, many industrial, commercial, and residential buildings were designed and built using moment frames. But the occurrence of the 1994 Northridge earthquake challenged this misconception. After that, it was observed that the beam to column connections of many buildings experienced a brittle fracture, and many steel buildings constructed with a moment frame could not provide the expected performance.

In order to investigate the seismic performance of

Drilled Flange plate connections, Maleki et al. applied the Incremental Dynamic Analysis (IDA), and the suitable seismic response of these connections was proved [2]. One of the most important components of the steel moment frame is its connections, and the most important issue in the rigid moment connection is how to transfer the moment to structural elements. In the moment frame, the beams should be able to provide the bending and shear capacity required to withstand gravity and lateral forces throughout the length of the beam. In moment frames, beams are usually considered as structural members that should be able to reach plastic moment values through their large plastic rotations, consequently, dissipating the earthquake-induced energy properly. For this purpose, the local buckling of the web and flange as well as their lateral-torsional buckling should be delayed to prevent early fracture of the member caused by instability. Therefore, only structural members with a compact section can be used as members that are expected to form a plastic hinge. Moreover, in these members, sufficient lateral bracings spaced at certain distances must be provided for both flanges in the location of the plastic hinge formation. Such patterns are made for the following reasons: during the earthquake, the upper and lower beam flanges are alternately subjected to the compression and the exact location of the plastic hinge formation is not known due to different loading conditions. Local buckling of the webs and flanges, as well as the lateral-torsional buckling of the member in the very large plastic rotations (at least in the conventional structural members), are inevitable. However,

*Corresponding author's email: mzahrai@ut.ac.ir



observing above mentioned regulations would postpone the progress of the strength reduction process, as a result, making possible the correct inelastic energy dissipation. Therefore, the continuity plates, panel zone sheets, and their connections provide the conditions for the transfer of moments from beam to the column in the moment frames of the lateral load-bearing systems, and any failure in this path questions the assumption of moment-resisting connection between the beam and the column [3-4].

Atashzaban et al. studied the optimum case of drilling in the beam flange and showed that there are a proper location and pattern for honey ball drilling that can reduce the stress in the joint and improve the seismic performance of the joint [5]. Kazerani et al. studied the drilled beam to column connection. Their research showed that flange drilling reduces the stress in the joint and resulted in the better seismic performance of the joint [6]. Hedayat et al., in their research, drilled the beam flange next to the end of the radius in order to obtain the proper flexibility. Although in this method, the presence of the hole provided a significant shear capacity of the radius and the difficulty of the initial rotation, it caused an increase in the flexibility of the connection without reducing the connection strength [7]. Vetr and Haddad [8] conducted a series of experimental tests to investigate the seismic performance of DFC beam-column connections under cyclic loading. In their study, the DFC connections reached the expected full bending capacity and showed sufficient rotational stiffness and optimal rotational ductility. Farrokhi et al. (2009) have proposed a reduced plate section connection by drilling holes at cover plates to create an intentional weak point. DFC connections can shift the stress concentrations from the connection face and, therefore, eliminate unfavorable local beam failure modes that are observed in conventional RBS connections. Their investigation showed that DFC connections can significantly improve the ductility capacity of the typical RBS and WUF connection. Moreover, the performance of DFC connections seems to be less dependent on the weld root quality, since the major nonlinear mechanism takes place adjacent to the drilled holes [9]. Li et al. conducted research on the RBS connections. They proposed and confirmed a method for estimating the RBS bending strength by drilling in the lower flange. The results obtained from the tensile loading test showed the strength and superiority of the fracture mechanics capacity along with it [10-11]. Kim et al. (2002) have carried out 10 full-scale tests on the cover plate and flange plate reinforced steel moment connections. In these experiments, it was proved that the cover plate and gusset plate connections outperform other connections with diffusion weld. In none of those 10 tests, the brittle fracture was observed and the plastic rotation reached a range between 2.3% and 3.9% [12]. Ten years later, Tessa has performed more extensive studies on similar samples; the core topic in these studies was the seismic performance of beam-to-column connections (Tsai KC and Popov EP 1988) [13]. A few years later, Popov has carried out a number of experiments to study maximum load-carrying conditions on connections as well as the cyclic behavior of connections [14].

This paper aims to optimize the seismic performance of DFC beam-to-box column connections by performing parametric studies. The studied parameters include the type of hole pattern, number, and type of holes of beam flange and flange to web thickness ratio. For this purpose, plastic rotation capacity, bending capacity of the beam, and triaxial stress in drilled-flange beam to column connections are compared to WUF (Welded Unreinforced Flange) connections. Based on the results of the present study, the type and number of hole affect the ductility of connection significantly and decreases stress concentration in the area of connecting beam to the column. In addition, it results in changing the plastic joint from the area of beam-to-column connection and panel zone to the beam in drilled region reducing the possibility of brittle failure in the connection site.

2- Validation of the Numerical Models

To evaluate the validity of the models in the study, research which is done by Fanaei et al. (2019) has been used [15]. The process of performing and comparing the model is as follows. The model is presented in Fig. 1.

The selected model was three-dimensional. The model name is TSDFC-4. The thickness and width of the beam are 15 and 180 mm, respectively. The beam and column features are shown in Table 1.

The three-dimensional finite element model of the solid element type is an eight-node C3D8R reduced integral. The concrete used was self-compact concrete (SCC) with a compressive strength of 35 MPa.

The loading is shown in Fig. 2. The results from the moment-rotation graph are shown in Fig. 3.

In the present study, the results of numerical modeling using ABAQUS finite element software and those of the experimental model are closely consistent and the error percentage of which is calculated as less than 3%.

3- Finite Element Modeling Approach

To carry out the parametric studies, the parameters were considered as follows: flange to web thickness ratios: 1, 1.5, and 2; type of hole pattern in the beam flange: clock and direct; the number of holes: 1, 2, 3, 4 and 5; hole diameter: 40mm; distance between holes in direct and clock modes: 130 mm and 65 mm, respectively; the dimensions of the used beam and column: I500*250 * t_f * t_w and W400*400*15, respectively. The boundary conditions were as follows: for displacement, all nodes located on the top and bottom of the column were supposed fixed. Out-of-plane buckling was applied. The loading was applied as a displacement of 192mm at the end of the beam. The specimens were named as follows: DFC denotes the drilled flange beam to column connection and WU denotes those connections with no holes. The third letter represents the hole pattern: D for direct and H for Clock pattern. The first number represents the number of hole rows and the second number is the flange to the web thickness ratio. Parametric models and their dimensions are listed in Table 2. In this study, expressions 1, 2, 3, and 4 refer to the number of rows of holes on the flange of the beams.

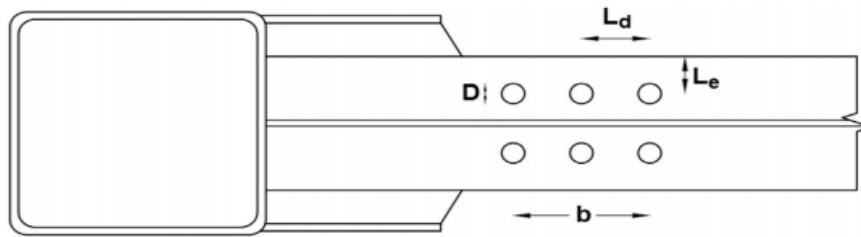


Fig. 1. Model selected for verification [15]

Table 1. Specifications of beams and columns used [15]

Model	Number of holes	Diameter of smallest hole (D_{min})	Diameter of biggest hole (D_{max})	Distance between the first and last hole (b)	Center to center distance of holes	D_{min}/b_f	D_{max}/b_f	b/d_b
TSDFC-4	4	18	27	210	70	0.1	0.15	0.7



Fig. 2. Loading history for proof-of-concept test

4- Effect of the hole pattern on Von Mises stress contour

Von Mises stress contour of the parametric models for the flange to web thickness ratio of 1, 1.5, and 2 are shown in Fig. 4 to 9, respectively. The Von Mises stress contour and yielding zones indicate that in all models with the flange to web thickness ratio of 2, yielding enters the column zones in the beam to column connection.

According to previous research studies, the shortcomings in the direct perforated connection have been discussed at the stress distribution between the holes is not uniform. Therefore, by proposing a clock pattern, the stress was distributed over a larger area of the beam flange.

Of course, in the clock pattern, the yielding of the column

in the connection locations is much lower than the direct pattern regarding the flange to web ratio of 2. This could be proved by comparing Figs. 6 and 9.

As this ratio increases, the bending capacity of the beam increases, and it also prevents the local buckling of the beam flange, so it improves the beam behavior by increasing the thickness.

Moreover, in all models with no hole and those with direct hole pattern, the yielding zone includes beam, column, and beam to column connection. In all models with a clock hole patterns and for the model where the flange to web thickness ratio is 1 or 1.5, the yielding zones are limited to the beam flange and web at the location of holes.

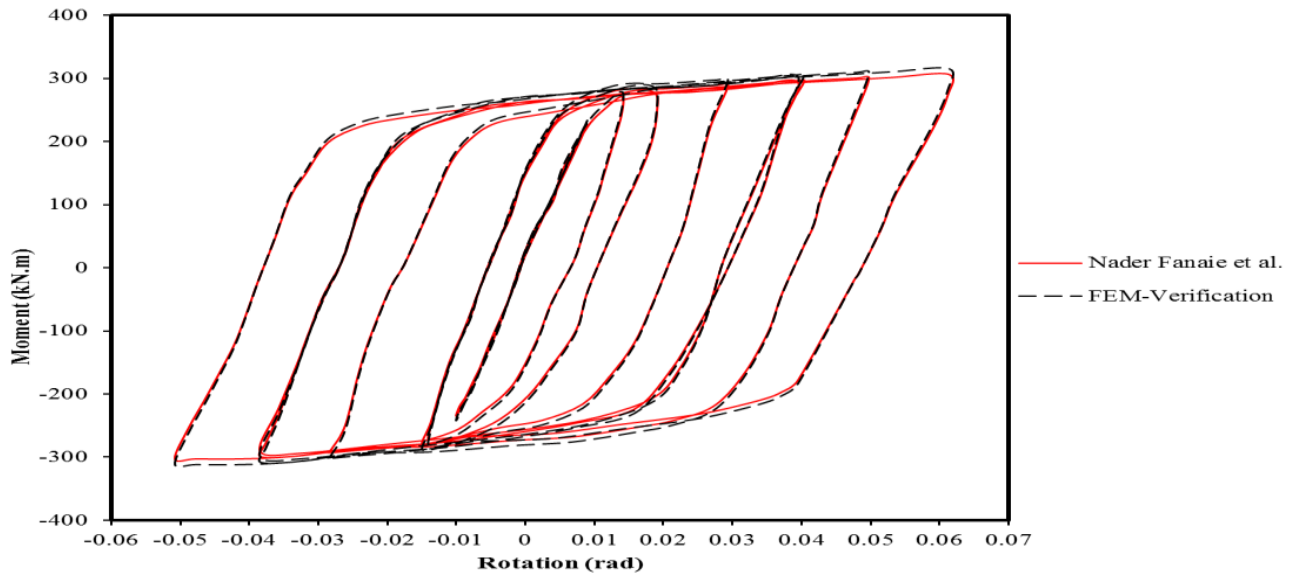
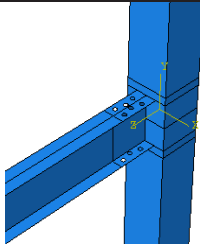
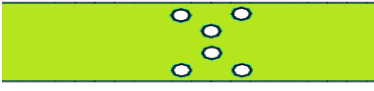
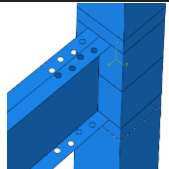

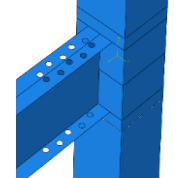
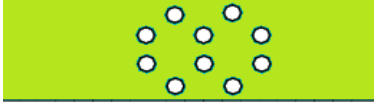


Fig. 3. Comparing moment-rotation curves between the current numerical work and Fanaie et al.

Table 2.a. Dimensions of the models with direct hole pattern used in the parametric study.

Model	Model shapes and Patterns of Drilled Flange	t_f/t_w	$t_f(mm)$	$t_w(mm)$
WU0		1	10	10
		1.5	15	10
		2	20	10
DFCD1		1	10	10
		1.5	15	10
		2	20	10
DFCD2		1	10	10
		1.5	15	10
		2	20	10
DFCD3		1	10	10
		1.5	15	10
		2	20	10
DFCD4		1	10	10
		1.5	15	10
		2	20	10

Table 2.b. Dimensions of the models with clock hole pattern used in the parametric study.

Model	Model shape	Patterns of Drilled Flange	t_f/t_w	t_f (mm)	t_w (mm)
DFCH3			1	10	10
			1.5	15	10
			2	20	10
DFCH4			1	10	10
			1.5	15	10
			2	20	10
DFCH5			1	10	10
			1.5	15	10
			2	20	10

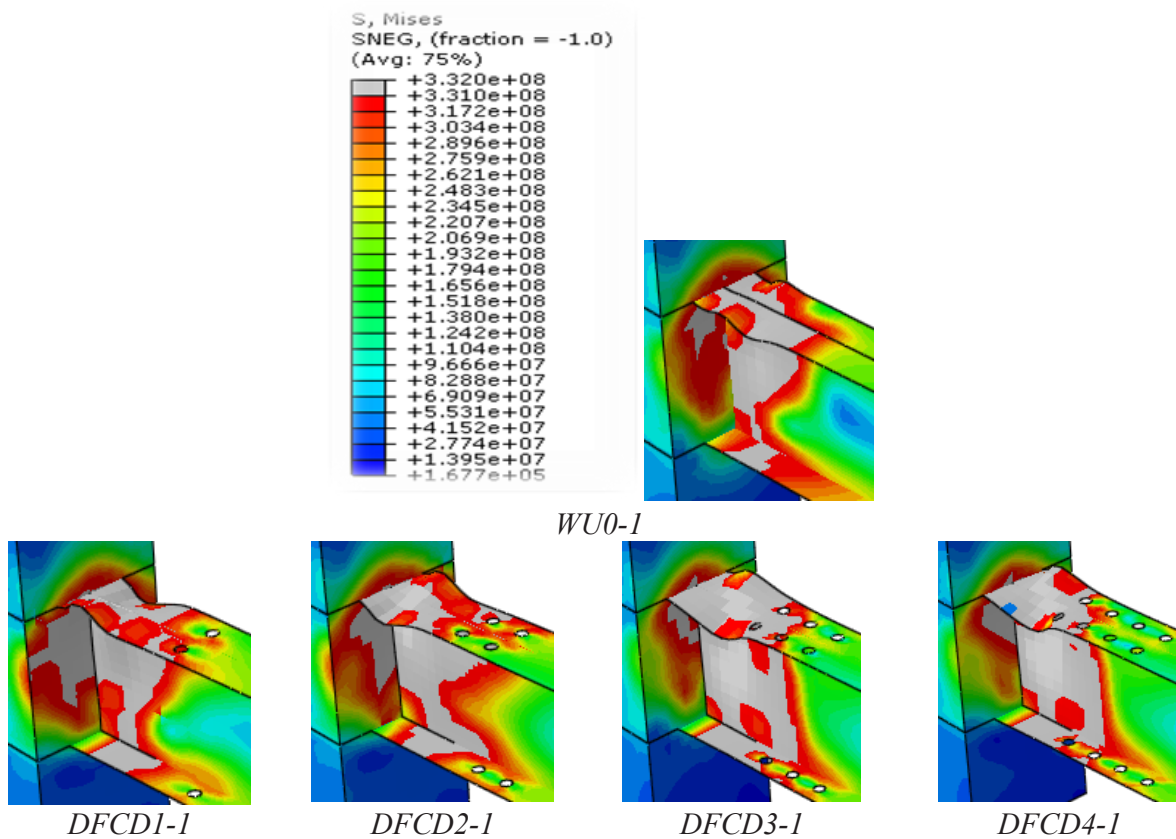


Fig. 4. Von Mises stress contours for those models with direct hole pattern and $\frac{t_f}{t_w} = 1$ (kN/m²)

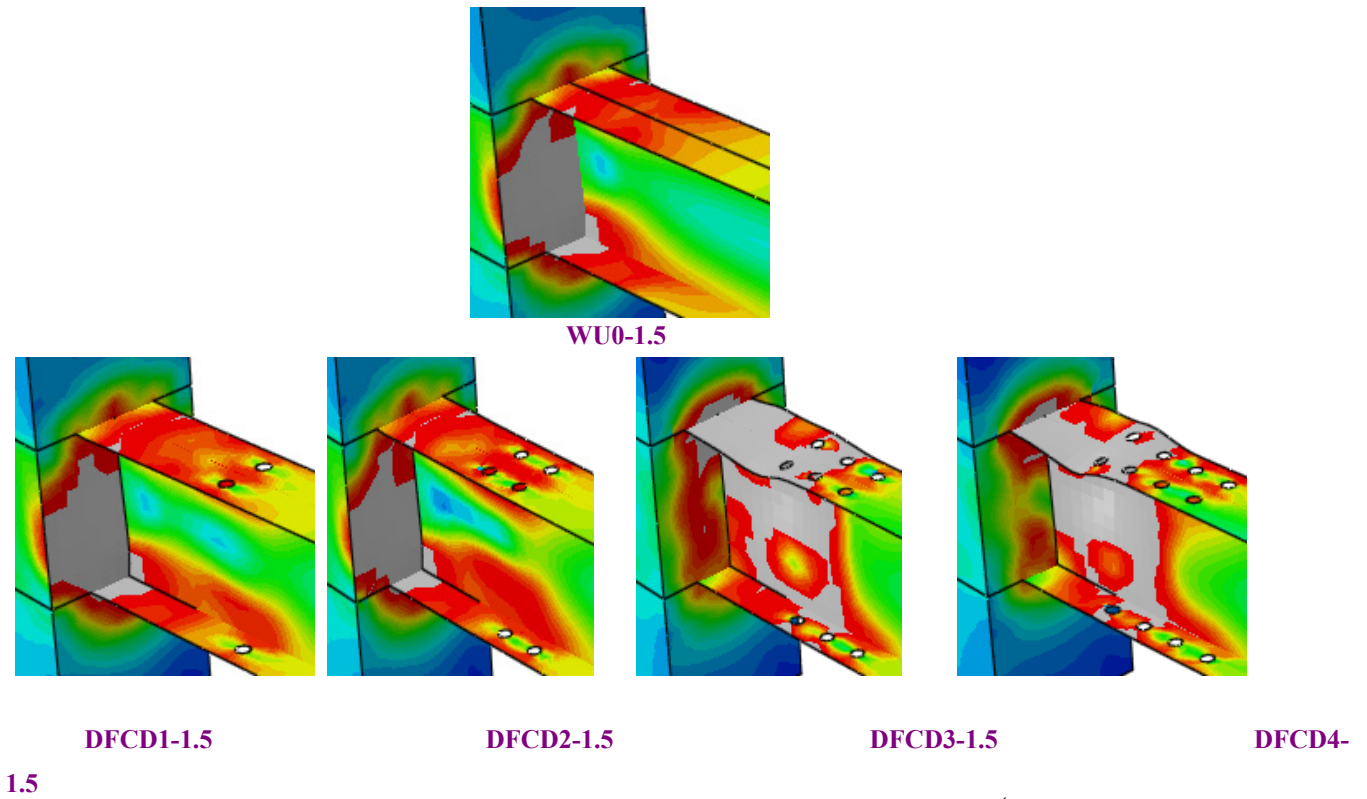


Fig. 5. Von Mises stress contours for those models with direct hole pattern and $\frac{t_f}{t_w} = 1.5$ (kN/m²)

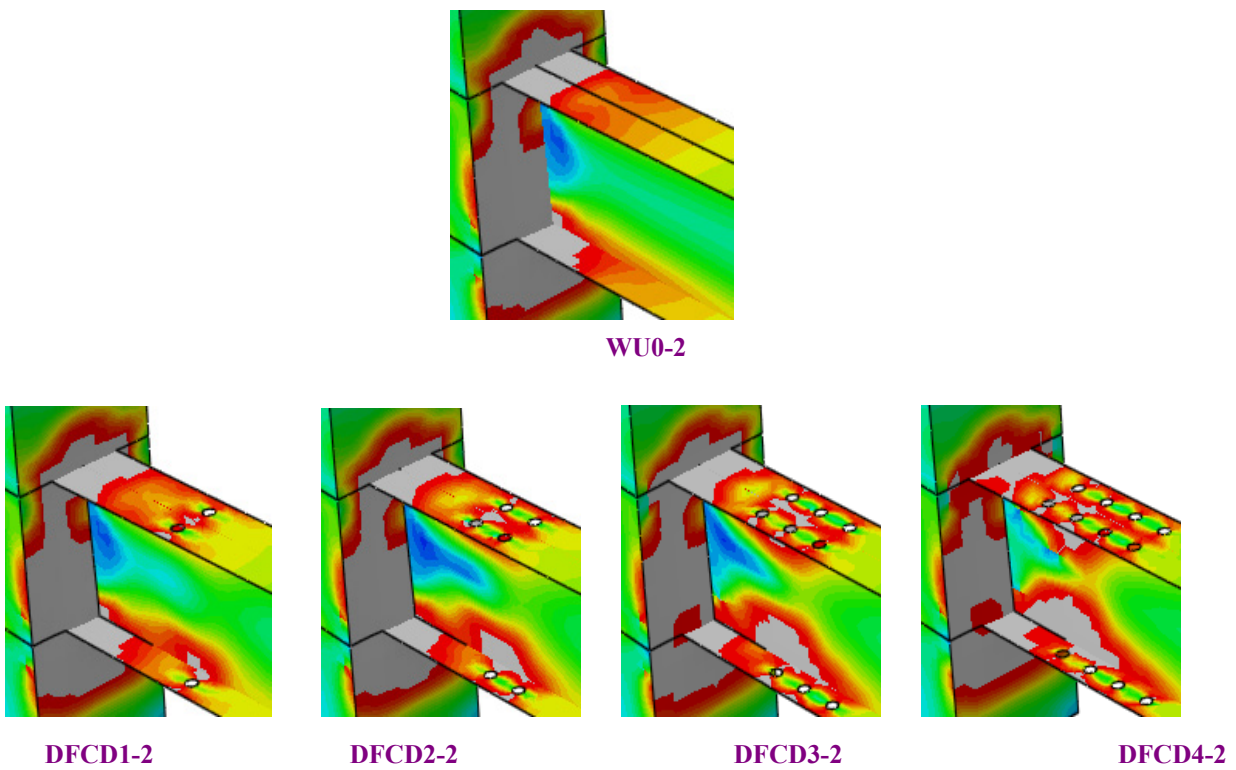


Fig. 6. Von Mises stress contours for those models with direct hole pattern and $\frac{t_f}{t_w} = 2$ (kN/m²)

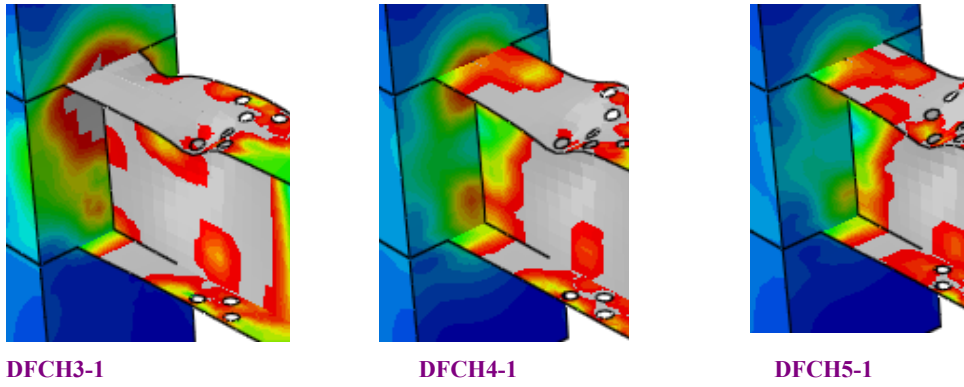


Fig. 7. Von Mises stress contours for those models with clock hole pattern and $\frac{t_f}{t_w} = 1$

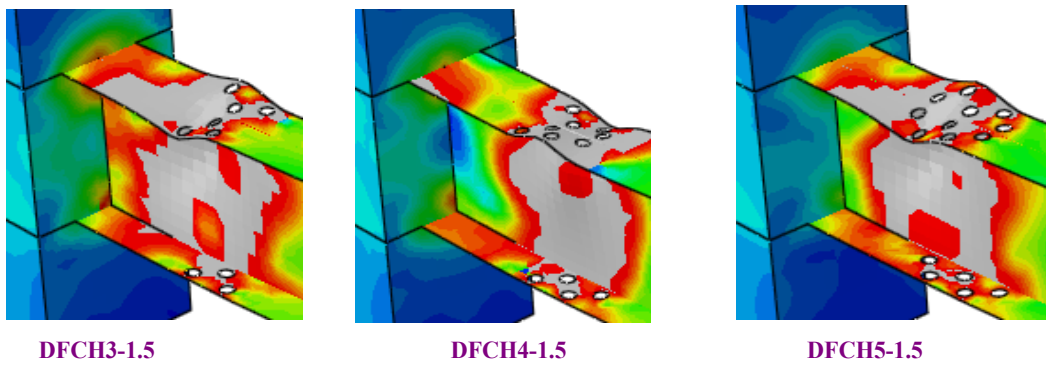


Fig. 8. Von Mises stress contours for those models with clock hole pattern and $\frac{t_f}{t_w} = 1.5$ (kN/m²)

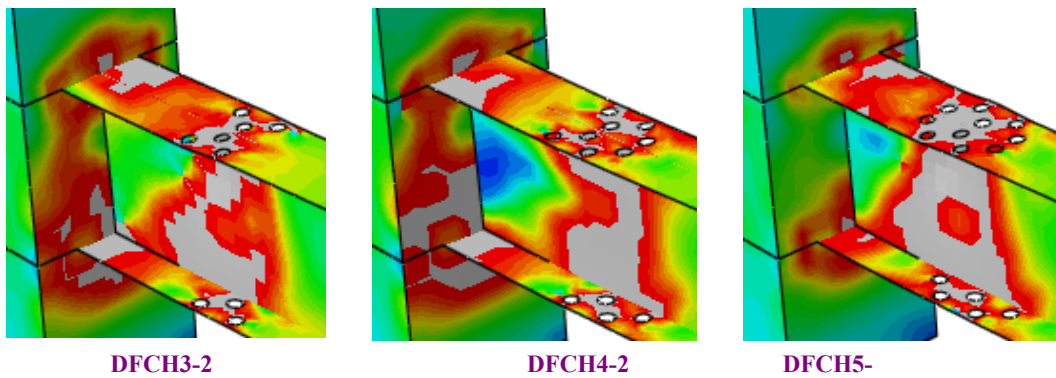


Fig. 9. Von Mises stress contour for those models with clock hole pattern and $\frac{t_f}{t_w} = 2$

5- Effect of hole pattern on maximum bending moment

The results of the maximum bending moment of finite element models and analysis of the plastic moment of the beams are shown in Table 3. To calculate the plastic moment, M_p , of the different steel sections, $M_p = Z F_y$ must be used. The average ratio of finite element results to analytical plastic moment is 1.01.

The results show that drilling a hole in the beam flange made no significant changes in the maximum bending capacity of the beams. The maximum variation in the beam bending capacity of a model with a hole to a model without hole is 7%.

6- Effect of the hole pattern on the moment-rotation curves

The bending moment-rotation curves for the beams are shown in Figs. 10 and 11. The results show that as the flange to web thickness ratio increases, the bending moment capacity increased. Also, as the flange to web thickness increased, the beam plastic rotation increases, indicating that ductility increases as well.

According to the bending moment and beam rotation diagrams, the maximum rotation of each pattern was specified. In these diagrams, in Fig. 12, the rotation variation with the

number of holes and 3 without holes has been shown for two types of the clock and direct holes. The results of the rotation in the maximum moment for the clock type hole showed that with the increase of the number of the holes, the rotation has also increased. Moreover, in the ratio of the thickness of beam flange to web equal to 1, the holes have caused the rotation decrease compared to the without-hole case. In the ratio of the thickness of flange to the web of beam equal to 1.5, with three rows of the hole, the maximum rotation has increased in such a way that the increasing process has continued up to 0.05 radians. Hence, it could be concluded that the flexibility has increased. Additionally, in the case of the flange to beam ratio equal to 2, because of the bending moment decrease and plastic joint shifting to the column, the maximum rotation for all the samples was equal and its amount was 6.4% radians. Regarding the direct pattern of the holes, the results showed that for the ratio of the thickness of flange to the web of beam equal to 1 and 1.5, the maximum rotation has decreased, thus, the flexibility decrease could be concluded. In the ratio of the thickness of beam flange to the web of equal to 2, as well, the maximum rotations for all the cases were equal and its amount was 6.4% radian, due to the bending moment decrease and plastic hinge shift to the column. Table 4 shows the values of connection stiffness and ductility.

Table 3. Plastic moment of the beams.

Model	M_{FEM} (using software)	$M_p = ZF_y$	$\frac{M_{FEM}}{M_p}$
WU0-1	586	577	1.02
WU0-1.5	800	790	1.01
WU0-2	988	1002	0.99
DFCH3-1	571	577	0.99
DFCH4-1	571	577	0.99
DFCH5-1	558	577	0.97
DFCH3-1.5	759	790	0.96
DFCH4-1.5	757	790	0.96
DFCH5-1.5	740	790	0.94
DFCH3-2	941	1002	0.94
DFCH4-2	953	1002	0.95
DFCH5-2	922	1002	0.92
DFCD1-1	576	577	1.00
DFCD2-1	552	577	0.96
DFCD3-1	588	577	1.02
DFCD4-1	574	577	0.99
DFCD1-1.5	816	790	1.03
DFCD2-1.5	811	790	1.03
DFCD3-1.5	802	790	1.01
DFCD4-1.5	790	790	1.00
DFCD1-2	988	1002	0.99
DFCD2-2	986	1002	0.98
DFCD3-2	984	1002	0.98
DFCD4-2	978	1002	0.98

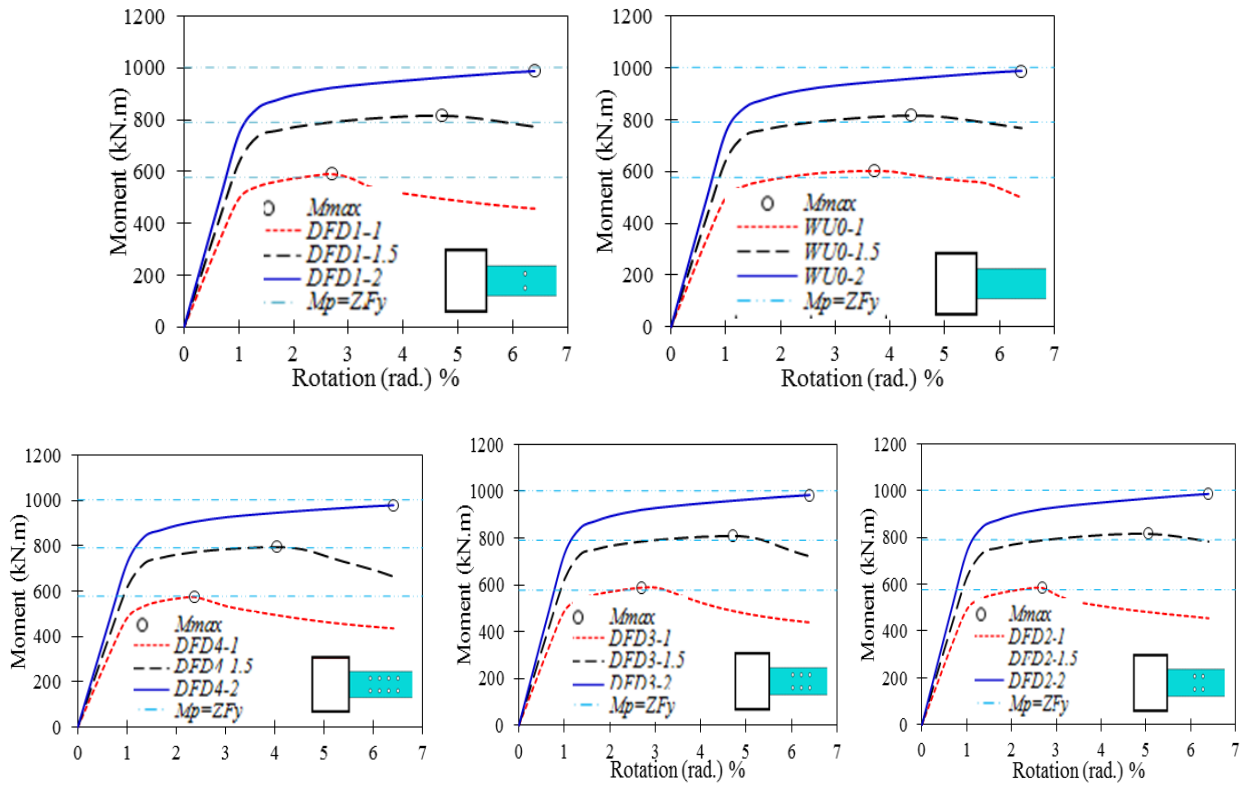


Fig. 10. Bending moment - rotation curve for beams with direct hole pattern.

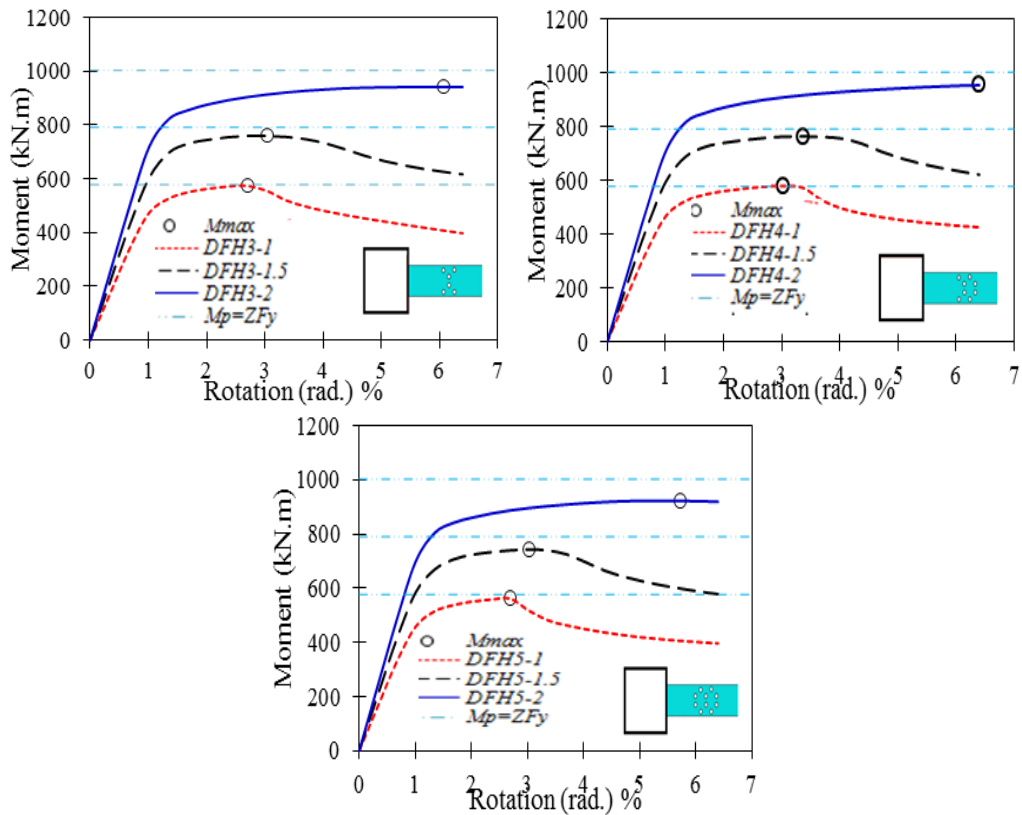
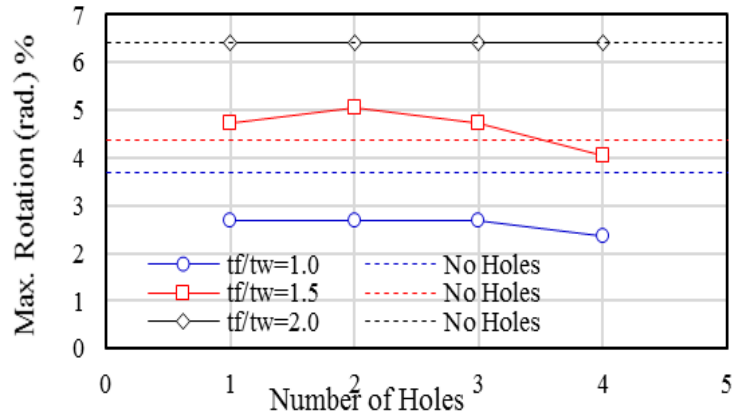
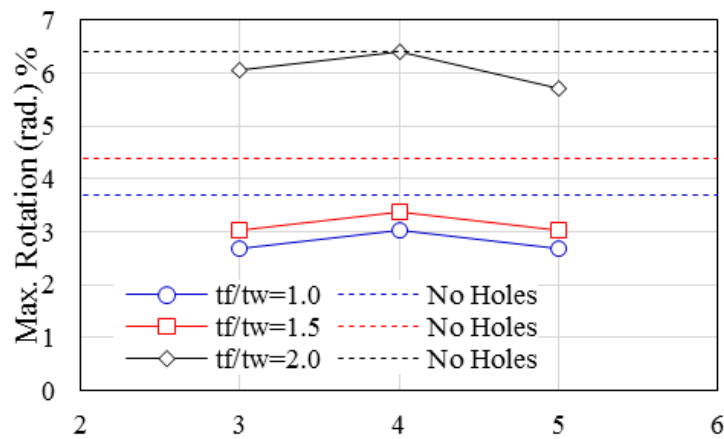


Fig. 11. Bending moment - rotation curve for beams with clock hole pattern.



(a)



(b)

Fig. 12.a. Variations of rotation for clock hole-pattern, b. Variations of rotation for direct hole-pattern.

7- Effect of the= hole pattern on the shear capacity of the panel zone

The design shear strength in the panel zone is referred to as R_n , where denotes the reduction coefficient and is equal to 0.9 and R_n denotes the nominal strength, which is determined according to the extreme shear yield as follows [16]. If the effect of the panel zone deformation is not considered in the structural analysis:

In a case where $P_u \leq 0.4P_c$:

$$R_n = 0.6F_y d_c t_w \quad (1)$$

In the case where $P_u > 0.4P_c$:

$$P_u > 0.4P_c : R_n = 0.6F_y d_c t_w \left(1.4 - \frac{P_u}{P_c}\right) \quad (2)$$

If the effect of the panel zone deformation is considered in the structural analysis, then:

In the case where $P_u \leq 0.75P_c$:

$$R_n = 0.6F_y d_c t_w \left(1 + \frac{3b_{cf} t_{cf}^2}{d_b d_c t_w}\right) \quad (3)$$

In the case where $P_u > 0.75P_c$:

$$R_n = 0.6F_y d_c t_w \left(1 + \frac{3b_{cf} t_{cf}^2}{d_b d_c t_w}\right) \left(1.9 - \frac{1.2P_u}{P_c}\right) \quad (4)$$

where, P_c denotes the axial force of column section, P_u is the axial strength required for the column, d_b is the height of

Table 4. stiffness and ductility of the studied models

Name	Stiffness (kN/Rad %)	ductility
DFCD1-1	55000	4.8
DFCD1-1.5	62400	3.85
DFCD1-2	67692.31	4.55
WU0-1	59000	5.5
WU0-1.5	71818.18	4.58
WU0-2	80000	5
DFCD4-1	55555.56	5.5
DFCD4-1.5	70909.09	4.58
DFCD4-2	84500	4.23
DFCD3-1	59000	5.5
DFCD3-1.5	71818.18	4.58
DFCD3-2	76818.18	4.23
DFCD2-1	58000	5.3
DFCD2-1.5	65833.33	4.42
DFCD2-2	70000	4.08
DFCH3-1	50000	4.91
DFCH3-1.5	58333.33	4.91
DFCH3-2	70000	4.15
DFCH4-1	55000	4.82
DFCH4-1.5	67272.73	4.58
DFCH4-2	76363.64	0.42
DFCH5-1	58000	5.2
DFCH5-1.5	58333.33	4.42
DFCH5-2	63076.92	4.15

the beam section, d_c denotes the height of the column section, t_{cf} is the column flange thickness, b_{cf} is the column flange width, t_w is the column web thickness. The shear capacity of the panel zone has been analyzed and the results are shown in terms of rotation of the panel zone in Fig. 13. The shear capacity of the panel zone obtained from the analysis is 3348kN. Moreover, the shear capacity of the panel zone was calculated using the equation (3) presented in the AISC seismic design manual [16]. It was calculated as 3257 kN. The ratio of the panel zone capacity obtained by the finite element method to the one obtained according to the AISC guide is 1.01. The results obtained from the investigation of the panel zone show that in none of the models, the panel zone has not reached the plastic rotation; therefore, no changes in the shear capacity of the panel zone were observed in the case of direct hole pattern or the case without the hole.

8- Investigating the connection behavior under cyclic loading

In the previous section, the non-linear behavior of the intended models was studied under static loading. Accordingly, the non-linear behavior of these models was studied under cyclic loading and the cyclic diagrams, which were among the best criteria for characterizing the non-linear reciprocating behavior of the structure under study. The cyclic loadings were under the AISC loading protocol and were applied to the end of the beam. In Fig. 14, this pattern has been shown.

In Fig. 15, the displacement is selected relative to the maximum displacement drift, and at each stage, a percentage of it is considered to reach the maximum displacement value at the end. The loading history was selected based on the recommendations presented in AISC 341-10 [14] and the SAC/BD-97/02 loading protocol as illustrated in Fig. 14[17].

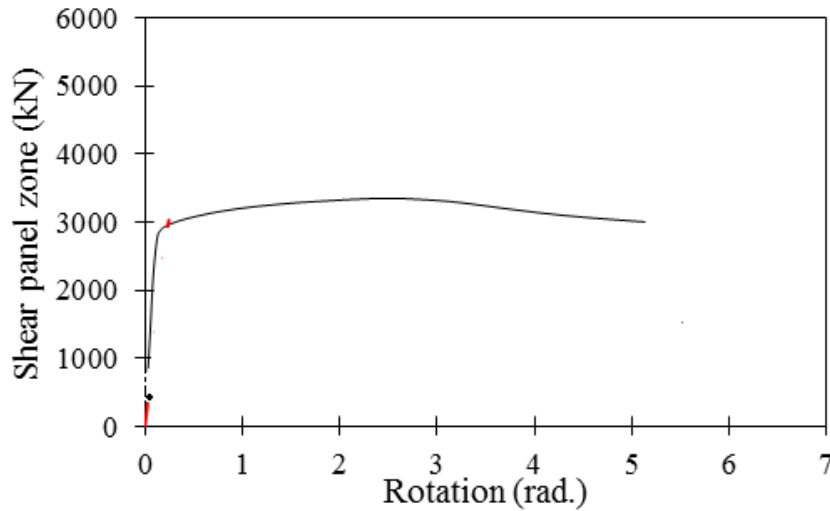


Fig. 13. Analytical shear capacity of the panel zone curve versus rotation.

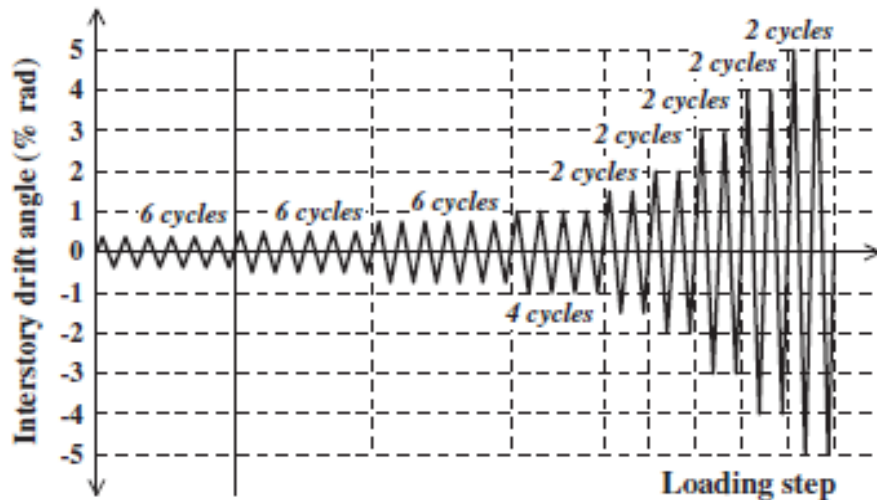


Fig. 14. Cyclic loading protocol.

In Fig. 15, the Von-Mises stress counter and the yielded area are shown for WU0-1.5, DFCH3-1.5 and DFCD3-1.5 models. They showed that in the clock pattern under these loading, they have performed better and the plastic joint and the yielded area were more in the drilled area. In Fig. 16, the hysteresis (cyclic) diagrams of the WU0-1.5, DFCH3-1.5, and DFCD3-1.5 models have been studied. According to these diagrams, the absorbed energy in the clock pattern was clearer in such a way that the energy adsorption in the WU0-1.5, DFCH3-1.5, and DFCD3-1.5 models were 178484.9, 223306.6, and 196693.3, respectively. According to Fig. 16, it can be observed that the area below the DFCH3-1.5 model diagram is larger than those of the other

models. Also, the stress distribution in the figure DFCH3-1.5 compared to those two models WU0-1.5 and DFCD3-1.5 occurred from a higher surface on the flange of the beam.

9- Conclusion

In this study, from one row of holes to finally five rows of holes have been studied. As a result, the range of these holes is 192 mm to 712 mm above the column. The results show that the greater the number of holes and the greater the distance from the column, the amount of stress distribution in the holes will be from the first and second rows and will have little effect in the farther holes.

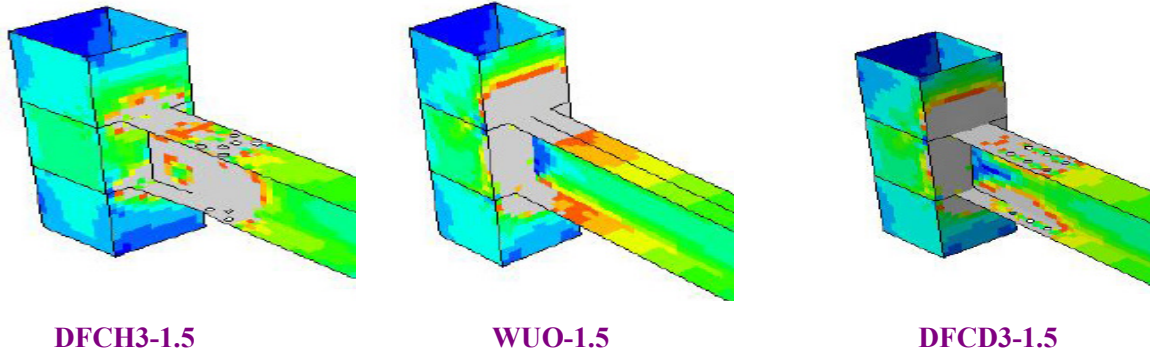


Fig. 15. Von Mises stress contours for three WU0-1.5, DFCH3-1.5 and DFCD3-1.5 models.

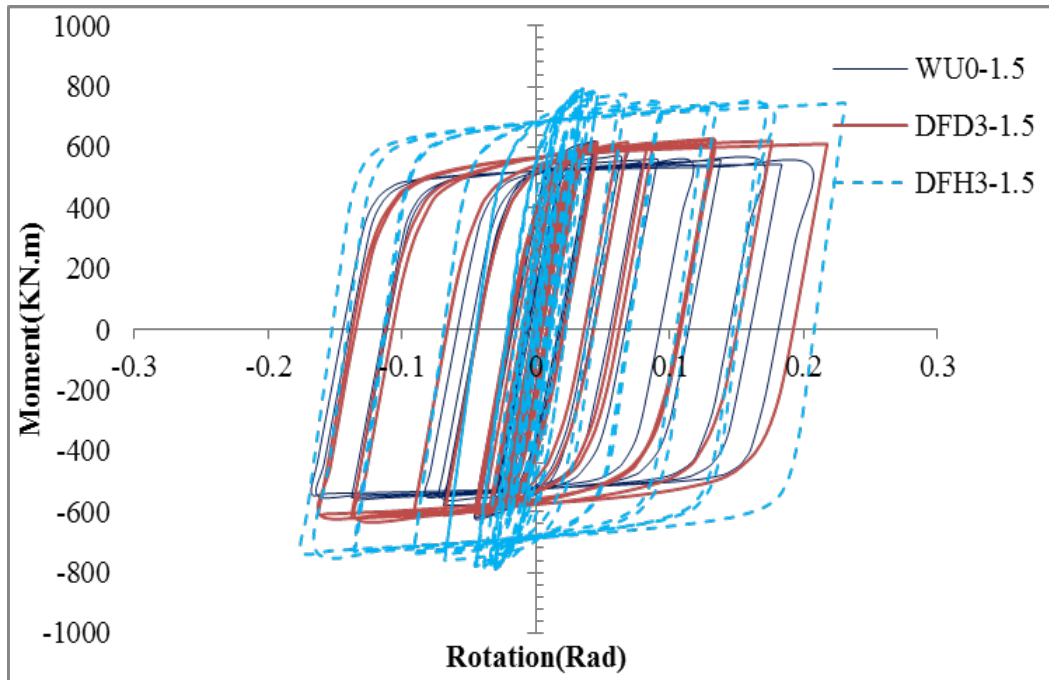


Fig. 16. The cyclic diagrams of WU0-1.5, DFCH3-1.5 and DFCD3-1.5 models.

In this study, according to the specifications considered for the models, the connection with the three holes of both models had better behavior including hysteresis diagram, stress distribution, and plastic joint formation, strength, and stiffness.

In the one-hole model, the stress concentration was around the same hole, which weakened the connection and reduced the strength and stiffness of the connection behavior. In the model with two holes, the behavior was slightly better than that with one hole. Therefore, in this study, it has been observed that the distance of the holes from the column from 192 to 582 mm and the application of more than one row of

holes lead to the optimal behavior at the joint.

In parametric studies, 24 models with different flange to web thickness ratios, hole patterns, and the number of holes in the beam flange were considered. The results of this research are as follows:

- 1-The results of moment-rotation curves show that the clock hole pattern provides better behavior than the clock hole pattern. Moreover, in the models with two to three rows of holes in the clock pattern, more optimal results were obtained.
- 2-The numerical results of Von Mises stress contour and yielding zones show that in models with a flange to web

thickness of 2, the yielding zone entered into the beam to column connection. Moreover, in all the models with no hole and those with direct hole patterns, the yielding zone includes beam, column, and beam to column connection. In all models with no hole and those with a clock hole pattern and for the case where flange to web thickness ratio is 1 or 1.5, the yielding zones are limited to the beam flange and web at the location of holes. Also in the models with clock hole pattern and the flange to web thickness ratio of 2, yielding zones are limited to beam flange and web at the location of holes as well as column and the beam to column connection. Also, the results indicate that the holes make the displacement of the plastic hinge from the beam to the column connection to the surface of the beam.

- 3-According to the cyclic diagrams, the clock pattern had more energy adsorption compared to the direct pattern and the one without a hole. Moreover, the cyclic curves enjoyed more symmetry.
- 4-The comparison of the bending moment- beam rotation curves show that as the beam flange to web thickness ratio increases, the capacity of the bending moment increases, and the beam rotation increases, indicating increased ductility.
- 5-The results of the maximum bending moment of finite element models and the one obtained from the equation used for the analysis of the plastic moment of the beam indicate that their difference ratio is 1.01. The results show that the creation of a hole in the flange of the beam does not have a significant change in the bending capacity of the maximum beams. The maximum variation in the beam bending capacity of a model with a hole to a model without a hole is 7%. Moreover, as the number of holes increases in the beam flange, the bending capacity of the beams decreases.
- 6-The investigation of the panel zone shows that in none of the models the panel zone has reached the plastic rotation. It is due to plastic hinge formation in the beam in the models with drilled flange and the plastic hinge formation in the beam and the beam to the column connection in the models with no holes.

10- Nomenclature

b = Distance between the first and last hole

D = Diameter of hole

d_b = Height of the beam section

d_c = Height of the column section

F_y = Yield stress

M_{FEM} = Moment by finite element method

M_p = Plastic Moment Capacity

P_c = Axial force of column section

P_u = Axial strength required for column

R_n = Nominal strength

t_f = Flange thickness

t_w = Web thickness

Z = Section plastic modulus

References

- [1] G. Pachideh, M. Gholhaki, A.S. Daryan, Analyzing the damage index of steel plate shear walls using pushover analysis, in: Structures, Elsevier, 2019, pp. 437-451.
- [2] Maleki, R.A. Jazany, M.S. Ghobadi, Seismic fragility assessment of SMRFs with drilled flange connections using ground motion variability, KSCE Journal of Civil Engineering, 23(4) (2019) 1733-1746. Engineering, Vol.23, No.4, pp.1733-46.
- [3] A. Karimian, A. Armaghani, A. Behraves, Performance of Low-yield Strength Plates in Beam-column Connections against Progressive Collapse, KSCE Journal of Civil Engineering, 23(1) (2019) 335-345.
- [4] M. Gholhaki, G. Pachideh, Investigating of damage indexes results due to presence of shear wall in building with various stories and spans, Int J Rev Life Sci, 5(1) (2015) 992-997.
- [5] A. Atashzaban, I. Hajirasouliha, R.A. Jazany, M. Izadinia, Optimum drilled flange moment resisting connections for seismic regions, Journal of Constructional Steel Research, 112 (2015) 325-338.
- [6] S. Kazerani, N. Fanaie, S. Soroushnia, Seismic behavior of drilled beam section in moment connections, Journal of Numerical Methods in Civil Engineering, 1(4) (2017) 1-6.
- [7] A.A. Hedayat, H. Saffari, M. Mousavi, Behavior of steel reduced beam web (RBW) connections with arch-shape cut, Advances in Structural Engineering, 16(10) (2013) 1645-1662.
- [8] M. Vetr, A. Haddad, Study of drilled flange connection in moment resisting frames, in: Report No. 3732, International Institute of Earthquake Engineering and Seismology Tehran; Iran, 2010.
- [9] H. Farrokhi, F. Danesh, S. Eshghi, A modified moment resisting connection for ductile steel frames (Numerical and experimental investigation), Journal of Constructional Steel Research, 65(10-11) (2009) 2040-2049.
- [10] S.J. Lee, S.E. Han, S.Y. Noh, S.-W. Shin, Deformation capacity of reduced beam section moment connection by staggered holes, in: International conference on sustainable building, Seoul, Korea, 2007.
- [11] T. Kim, A. Whittaker, A. Gilani, V. Bertero, S. Takhirov, Experimental evaluation of plate-reinforced steel moment-resisting connections, Journal of structural engineering, 128(4) (2002) 483-491.
- [12] S.J. Lee, S.E. Han, S.Y. Noh, S.-W. Shin, Deformation capacity of reduced beam section moment connection by staggered holes, in: International conference on sustainable building, Seoul, Korea, 2007.
- [13] B. Stojadinović, S.C. Goel, K.-H. Lee, A.G. Margarian, J.-H. Choi, Parametric tests on unreinforced steel moment

- connections, *Journal of Structural Engineering*, 126(1) (2000) 40-49.
- [14] K.-C. Tsai, E.P. Popov, *Steel beam-column joints in seismic moment resisting frames*, University of California, Berkeley, 1988.
- [15] H. Krawinkler, E.P. Popov, V.V. Bertero, Shear behavior of steel frame joints, *Journal of the Structural Division*, 101(11) (1975) 2317-2336.
- [16] N. Fanaie, H.S. Moghadam, Experimental study of rigid connection of drilled beam to CFT column with external stiffeners, *Journal of Constructional Steel Research*, 153 (2019) 209-221.
- [17] AISC 341-10. (2010). "Seismic Provisions for Structural Steel Buildings, Chicago (IL): American Institute of Steel Construction."
- [18] SAC. SAC/BD-97/02 Version 1.1, Protocol for fabrication, inspection, testing, and documentation of beam-column connection tests and other specimens, Sacramento (CA): SAC Joint Venture, 1997.

HOW TO CITE THIS ARTICLE

M. Vajdian, S. M. Zahrai, S. M. Mirhosseini, E. Zeighami, Cyclic Behavior of Various Drilled Flange Beam Connected to Box Column, *AUT J. Civil Eng.*, 5(1) (2021) 79-94.

DOI: [10.22060/ajce.2020.17448.5633](https://doi.org/10.22060/ajce.2020.17448.5633)



